Analysis of Methane-Air Edge Flame Structure

Habib N. Najm[1], Mauro Valorani[2], Dimitris A. Goussis[3], and F.Creta[2]

[1]Sandia National Laboratories, Livermore, CA 94550,
[2]University of Rome "La Sapienza", Rome, Italy,
[3]National Technical University of Athens, Greece

Abstract

We compute a methane-air edge flame stabilized in a prescribed two-dimensional mixing layer using detailed chemistry and transport. We study the internal structure of this flame using Computational Singular Perturbation analysis. The analysis outlines the variation of the driving time scale and the number of exhausted modes within the edge flame, revealing significant internal structure. We use these results to outline key pathways of fuel oxidation in the lean, rich, and stoichiometric regions of the edge flame. This information provides the basis for identification of simplified chemical mechanisms suitable for this configuration.

Introduction

Edge flames can be encountered in many reacting flow configurations in which partial premixing of fuel and oxidizer occurs [1, 2]. The symmetric, tribrachial, edge flame structure is typically observed in flows with a uniform incoming velocity profile and/or a symmetrical/slowly-varying mixture-fraction field topology. Both bibrachial and monobrachial edge flames are also observed [2]. There has been a growing number of experimental, analytical and numerical studies of edge flames [3, 4]. The reviews by Buckmaster [1] and Chung [2] provide a broad overview of the history and recent developments in the study of edge flames.

In the present work we analyze the internal structure of a methane-air edge flame using Computational Singular Perturbation (CSP) theory [5, 6]. We also use CSP for automated generation of simplified chemical models. CSP enables automatic identification of fast and slow reaction processes in chemical models, and the decoupling of fast-exhausted/dormant modes from the slow modes that drive the time evolution of the chemical system. The method relies on the identification of a suitable set of basis vectors that enable the decoupling of fast and slow processes. A leading-order approximation of these vectors is provided by the eigenvectors of the Jacobian of the chemical source term.

In the present work, we compute a methane-air edge flame stabilized against a prescribed uniform-velocity mixing layer using detailed chemistry (GRImech3.0 [7]) and transport. CSP analysis of the computed flame structure highlights the spatial variation of the driving time scale and the number of exhausted M over the edge flame, revealing interesting internal structure. We also use CSP to identify key fuel oxidation pathways that are dominant in the lean, rich, and stoichiometric regions of the edge flame, thereby constructing corresponding simplified reaction graphs. In the following, we outline the setup of the problem, then present the analysis of the edge flame using CSP, followed by the simplified mechanism graphs. We finish with conclusions summarizing the main findings of the work.

1   Problem Setup

We consider a methane-air edge flame in two-dimensions (2D) stabilized against an incoming mixing layer flowfield with a uniform inflow velocity profile. The computational model includes the low Mach number approximation, and employs GRImech3.0 [7] kinetics and mixture-averaged transport. The inflow is specified with a uniform velocity and a hyperbolic-tangent mixture-fraction profile, going from pure air on one side of the domain to pure CH_4 on the other. The edge flame structure is illustrated in Figure 1. The figure shows the spatial distribution of the CH_4 and O_2 fields, exhibiting significant leakage of O_2 into the fuel stream. Also shown is the temperature profile, exhibiting the expected fast temperature rise at the edge flame tip, followed by the non-premixed trailing flame high-temperature ridge. We also show the heat release rate, which exhibits a characteristic bibrachial edge flame structure with a premixed lean flame branch extending

towards the oxidizer stream and a non-premixed flame branch extending upwards towards the domain exit. The rich branch is folded into the non-premixed flame structure behind the edge flame. Given O_2 leakage, the true non-premixed flame structure is not retrieved until the leaked oxidizer is exhausted further downstream.

2   CSP Analysis of the Edge Flame

We studied the edge flame structure using CSP. Key results are illustrated in Figure 2 showing the edge flame and a part of the trailing flame. Frame (a) in the figure shows the spatial distribution of the driving time scale τ_{M+1}, being the time scale at which the chemical system evolves locally. Clearly τ_{M+1} is largest in the unburnt cold mixture, as would be expected from the frozen chemical activity in this region. As the edge flame is approached, τ_{M+1} decreases, reflecting the activation of chemical processes. We note a non-trivial structure in this region with non-monotonous variation of τ_{M+1} as the edge flame is approached. There is also significant structure within the edge flame region itself. The region with smallest τ_{M+1} is clearly at the front-end of the edge flame and on the fuel-side of both the edge flame and the trailing flame. This observation makes sense given the relevance of fast reactions in fuel-breakdown pathways. Significant fuel-breakdown activity is expected at the front of the edge flame. Moreover, very little of this is expected on the oxidizer side given the lack of fuel on this side of the flame, as seen in Fig. 1. On the other hand, such time scales are to be expected on the fuel side, stretching up along the partially-premixed flame, and towards the trailing non-premixed conditions further downstream. The edge flame region behind the lean-branch, and further downstream along the oxidizer side of the trailing flame, exhibits a zone of lower active time scales, consistent with expected slower chemical activity typical of oxidation reactions pursuant to fuel breakdown. There is some structure within this region, with a narrow band of faster time scales on the right-hand side of this region, signifying a gradual progression from the faster fuel-breakdown reactions to the slower oxidation reactions. Moreover, the figure indicates the presence of a very narrow band of slower active time scales whose topology includes the curved lean flame branch and the trailing flame region.

Frame (b) in Fig. 2 shows the spatial distribution of the number of exhausted modes M. To a large extent we see a structure here that mirrors that of the active time scale. Broadly, lower values of M are observed within the edge flame and the trailing flame structure. Moreover, as observed for τ_{M+1}, two distinct high-M features are evident within the edge flame region, a broader one on the oxidizer side, and a much narrower one, to its right, within the trailing flame. In fact, this narrow feature coincides with the ridge of peak temperature going downstream in the trailing flame (not shown). Moreover, frame (c) indicates that the broader feature on the oxidizer side is associated with a region of peak O-atom mass fraction, again consistent with the dominance of oxidation reactions. On the other hand, frame (d) illustrates that the high OH ridge roughly straddles both features. Finally, the bottom right frame presents compelling evidence that the very narrow low-M/high-τ_{M+1} feature is associated with Nitrogen chemistry, as a ridge-peak of N-atom mass fraction coincides very well with this feature.

3   Identification of Prevailing Fuel Oxidation Pathways

As discussed in [8], a by-product of the procedure required to generate simplified (skeletal) kinetic mechanisms is the identification of the so-called active species and reactions at any prescribed spatial and temporal location. We used the techniques of [8] to identify the prevailing oxidation mechanisms of the fuel in the present edge flame. We selected locations typical of lean, stoichiometric, and rich oxidation conditions, respectively. The chemical mechanism graphs obtained at these locations are shown in Fig. 3. The arrows proceed from reactants to products moving from left to right; above the arrow one finds the reaction number and the oxidant species appearing in that reaction. Visual inspection of the graphs allows the discrimination between key oxidation pathways of the fuel; it is apparent that at lean conditions CH_4 is first attacked by OH, and then converted into CO_2 via the sequence: {R#98:OH+CH_4 → CH_3+H_2O; R#10:O+CH_3 → H+CH_2O; R#101:OH+CH_2O → HCO+H_2O; R#168:HCO+O_2 → HO_2+CO; R#99:OH+CO → H+CO_2}. On the other hand, at rich condition, CH_4 is first attacked by H, and then converted into the intermediates products CO, C_2H_6, and C_2H_2 according to the three paths, respectively: (1) for CO: {R#53: H+CH_4 →

CH_3+H_2 ; R#119: $HO_2+CH_3 \rightarrow OH+CH_3O$; R#382: $H+CH_2O(+M) \leftarrow CH_3O(+M)$; R#58: $H+CH_2O\rightarrow$ $HCO+H_2$; R#166: $HCO+H_2O \rightarrow H+CO+H_2O$; R#167: $HCO+M \rightarrow H+CO+M$; R#168: $HCO+O_2 \rightarrow$ HO_2+CO }, and, (2) for C_2H_6: {R#158: $2CH_3(+M)\rightarrow C_2H_6(+M)$}, and (3) for C_2H_2: {R#159: $2CH_3 \rightarrow$ $H+C_2H_5$; R#399: $H+C_2H_4(+M) \leftarrow C_2H_5(+M)$; R#75: $H+C_2H_4 \rightarrow C_2H_3+H_2$; R#396: $H+C_2H_2(+M)$ $\leftarrow C_2H_3(+M)$}.

Finally, at stoichiometric conditions, CH_4 is attacked by both H and OH and converted into CH_3 via R#53 and R#98. Next, CH_3 is consumed via two paths; one path leading to HCO via R#10 and R#58 with HCO converted into CO by R#166, R#167, and R#168, and the other path to HCCO, via R#158 and {R#78: $H+C_2H_6 \rightarrow C_2H_5+H_2$; R#113: $OH+C_2H_6 \rightarrow C_2H_5+H_2O$}, R#399, R#396, and {R#21: $O+C_2H_2$ $\rightarrow H+HCCO$}, with HCCO converted into CO by {R#176: $HCCO+O_2 \rightarrow OH+2CO$; R#79: $H+HCCO$ $\rightarrow CH_2(S)+CO$ }.

Although some of these results are well expected, it is noteworthy that they have been recovered through an algorithmic procedure not requiring any expert intervention. We have found similar results for the oxidation of O and N at the regions of peak values of O and N, which are omitted here for reasons of brevity.

4   Conclusions

We have computed a bibrachial methane-air edge flame using detailed chemistry and transport, and analyzed its structure using CSP. Results outlined the spatial variation of driving time scales and the number of exhausted modes, highlighting significant structure within the edge flame. We also identified dominant chemical pathways in different regions of the edge flame, with associated simplified chemical mechanisms. Results highlight the utility of CSP for elucidating flame structure and generating simplified chemical models.

5   Acknowledgements

References

[1] Buckmaster, J., *Progress in Energy and Combustion Science*, 28:435–475 (2002).

[2] Chung, S.H., *Proceedings of the Combustion Institute*, 31:877–892 (2007).

[3] Amantini, G., Frank, J.H., Smooke, M.D., and Gomez, A., *Combustion and Flame*, 147:133–149 (2006).

[4] Takahashi, F., Linteris, G.T., and Katta, V.R., *Proceedings of the Combustion Institute*, 31:1575–1582 (2007).

[5] Lam, S.H., and Goussis, D.A., *Proc. Comb. Inst.*, volume 22, pp. 931–941, (1988).

[6] Goussis, D.A., and Lam, S.H., *Proc. Comb. Inst.*, volume 24, pp. 113–120, (1992).

[7] Smith, G. P., Golden, D. M., Frenklach, M., Moriarty, N. W., Eiteneer, B., Goldenberg, M., Bowman, C. T., Hanson, R. K., Song, S., Gardiner, W. C. Jr., Lissianski, V. V., and A., Qin, *www.me.berkeley.edu/gri_mech*, Version:3.0 7/30/99.

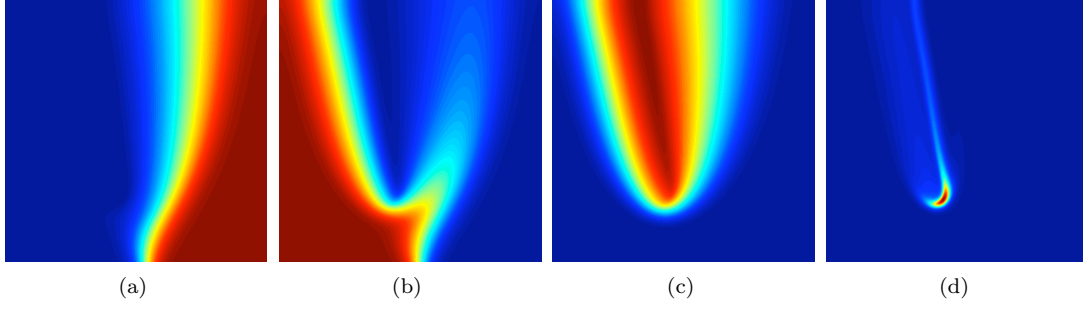[8] Valorani, M., Creta, F., Donato, F., Najm, H.N., and Goussis, D.A., *Proc. Comb. Inst.*, 31:483–490 (2007).

Figure 1: Edge flame structure: (a) CH_4 mole fraction, (b) O_2 mole fraction, (c) Temperature, and (d) heat release rate.
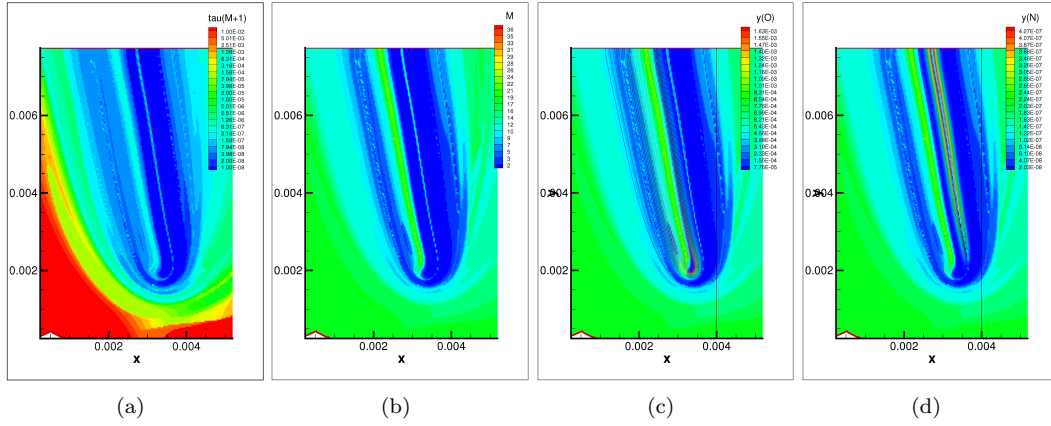

Figure 2: CSP analysis of the edge flame: (a) active time scale τ_{M+1}, (b) the number of exhausted modes M, (c) the contours of O superposed on the M-field, and (d) the contours of N superposed on the M-field.
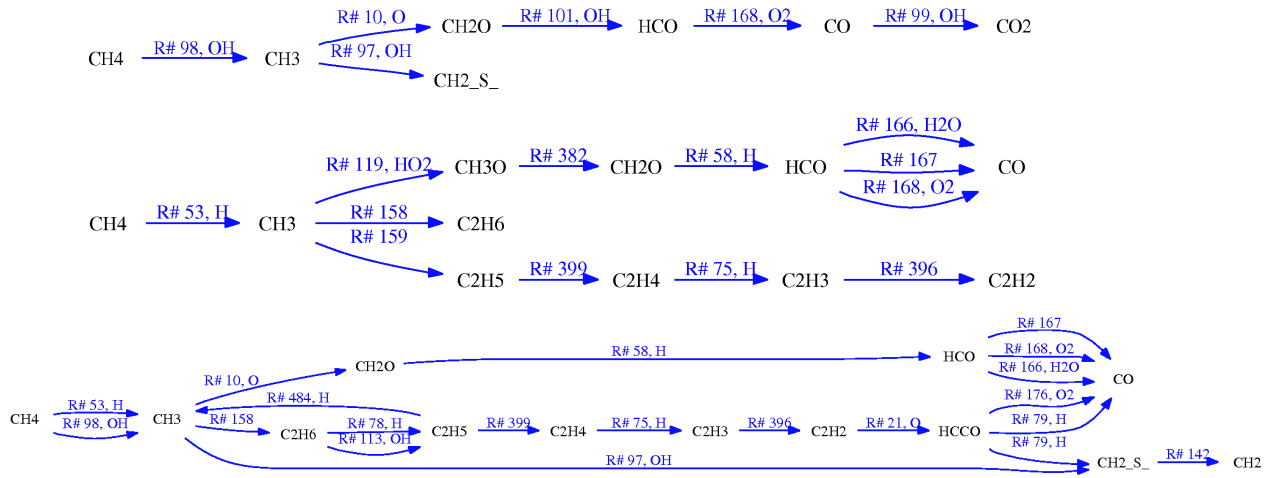

Figure 3: Prevailing kinetic pathways at lean (top), rich (mid), and stochiometric (bot) conditions.